



## Photocatalyst Activity of TiO<sub>2</sub>/CQD Nanocomposite for Degradating Pesticide Contaminants in Water

Asrianti Bt. Sunardi<sup>1</sup>, Kurnia Galuh Candra Kirana<sup>1</sup>, Erma Surya Yuliana<sup>1</sup>, Nandang Mufti<sup>1,2\*</sup>, and Hari Wisodo<sup>1</sup>

1. Department of Physics, Faculty of Mathematics and Natural Sciences, State University of Malang, Jl. Semarang 5, Malang 65145, Indonesia
2. Center of Advanced Materials and Renewable Energy, State University of Malang, Jl. Semarang 5, Malang 65145, Indonesia

\*E-mail: [nandang.mufti.fmipa@um.ac.id](mailto:nandang.mufti.fmipa@um.ac.id)

Received  
13 January 2022

Revised  
21 April 2023

Accepted for Publication  
23 September 2023

Published  
30 October 2023



This work is licensed under a [Creative Commons Attribution-ShareAlike 4.0 International License](https://creativecommons.org/licenses/by-sa/4.0/)

### Abstract

This study investigates the effectiveness of TiO<sub>2</sub>/CQD composites on the pesticide degradation. TiO<sub>2</sub>/CQD composites has been successfully synthesized using hydrothermal methods. The samples were characterized by XRD, TEM, PL, BET, and UV-Vis. The result of XRD shows the addition of CQD does not affect the crystal phase of TiO<sub>2</sub>. The result of TEM shows that CQD are well deposited on the TiO<sub>2</sub> surface. The particle size of the TiO<sub>2</sub>/CQD composite is getting larger after the addition of CQD compared to pure TiO<sub>2</sub> and the average particle size distribution is about 109-114 nm. PL analysis found that the addition of CQD increased the intensity of NBE emissions while Ti<sub>i</sub> decreased. The BET test result of the TiO<sub>2</sub>/CQD composite shows a surface area of 8.6710 m<sup>2</sup>/g. The pore diameter is 37.4 nm compared to pure TiO<sub>2</sub>. While the pore volume is 0.0754 cm<sup>3</sup>/g. Photocatalyst activity of TiO<sub>2</sub>/CQD against pesticides after 150 minutes of irradiation reached 89.9667%. TiO<sub>2</sub>/CQD photocatalyst has significant potential for pesticide water treatment. Further research is needed for large-scale optimization and evaluation.

**Keywords:** TiO<sub>2</sub>/CQD, Photocatalyst Activity, Pesticide Degradation

### 1. Introduction

Industrialization in Indonesia continues to increase, so facilities are needed to support the process's smooth running. One of the ways is improving the agricultural sector by providing facilities such as agricultural equipment, fertilizers, and chemicals including pesticides. Pesticides are chemicals used to prevent, control or eliminate pests on agricultural crops to increase productivity. Continuous use of pesticides can cause serious impacts on human, animal and plant lives [1]. Although useful for increasing agricultural production, excessive use of pesticides can harm the environment, animals, and especially humans [2]. It is known that pesticide exposure can cause birth defects, infertility, as well as endocrine and respiratory disorders in humans. In addition, small amounts of these residual compounds can irreversibly inactivate key enzymes in the central nervous system [1]. Therefore, a highly effective method to degrade pesticides is needed.

Photocatalysis is widely applied to industry because it is promising in wastewater treatment, air pollution control, production of hydrogen alloys, and carbon dioxide reduction. The abundant utilization of sunlight as an environmentally friendly energy source, ensures that the environment is not negatively impacted, but remains a viable energy source in the long term [3]. Semiconductor materials such as ZnO [4], TiO<sub>2</sub> [5], ZnS, and CuS for photocatalyst application [6]. TiO<sub>2</sub> is an ideal semiconductor material for photodegradation because it has good chemical stability, environmental friendliness, and relatively cheap price [7-8]. The TiO<sub>2</sub> bandgap is large (3.20 eV) and only works in the UV absorption area [9]. So that sunlight can be utilized optimally, TiO<sub>2</sub> must divert its absorption to the visible light area. In addition, TiO<sub>2</sub> is also easily subjected to electron-hole recombination [10]. A new alternative technique was recently developed with many advantages such as a simple, fast and low-cost methodology. In addition, it has sensors with high sensitivity, selection, and accuracy against various types of pesticides [1].

Carbon Quantum Dot (CQD) or Carbon Dot (CD) is a zero-dimensional (<10 nm) carbon-based nanomaterial known with small and strong size, manageable catalysis, and fluorescence characteristics [11]. In addition, CQD has a large absorption band, low toxicity, good chemical stability, and high optical absorption [12-13]. It makes CQD is the right candidate to improve the photocatalyst performance of TiO<sub>2</sub> materials. The addition of CQD can improve the TiO<sub>2</sub> response to visible light and resist electron-hole recombination [14]. By modifying TiO<sub>2</sub>/CQD, the potential to degrade organic compounds faster can be reached [15]. CQD can be applied in several fields, such as photocatalysis, nanomedicine, education and sensing [1, 11, 16]. The manufacture of TiO<sub>2</sub>/CQD composites for photocatalyst applications has been carried out by several researchers, including Tong et al, (2022) with synthesizing TiO<sub>2</sub>/CQD composites using the sol-gel hydrolysis method to degrade rhodamine B (RhB) in water obtained degradation rate of 85.47% [17]. Another TiO<sub>2</sub>/CQD composite was done by Mozdbar et al, with TiO<sub>2</sub>/CQD degradation performance shown 2.4 times under visible light compared to pure TiO<sub>2</sub> nanoparticles [18].

However, several studies that have been carried out are still used in powder form for photocatalysis treatment, which makes it difficult to separate the powder from the waste that has been processed. Therefore, it takes effort to make the separation process simpler and more efficient. The method that can be used to make photocatalyst material is an alternative photocatalyst membrane. TiO<sub>2</sub>/CQD composites are decomposed on the photocatalyst membrane and wastewater degradation testing is performed. In this study, the synthesis of TiO<sub>2</sub>/CQD composite will be carried out using hydrothermal methods. Photodegradation testing was carried out using 25 wp lannate pesticide waste. This study aims to examine the effectiveness and ability of TiO<sub>2</sub>/CQD photocatalyst in degrading pesticide contamination in water.

## 2. Method

### 2.1 Tools and Materials

The tools used in this study were autoclave, centrifuge tubes, drip pipettes, measuring cup (pyrex), beaker glass (pyrex), petri dish (pyrex), spatula, oven, digital balance, magnetic stirrer, hot plate stirrer, mortar and pestle, and centrifuge. The materials used in this study are titanium dioxide (TiO<sub>2</sub>), urea (CH<sub>4</sub>N<sub>2</sub>O<sub>7</sub>) (MERCK), citric acid (C<sub>6</sub>H<sub>8</sub>O<sub>7</sub>), ethanol PA (EtOH), distilled water, deionized water (ONELAB) purchased from Nurra Gemilang (Malang, Indonesia), pesticide lannate 25 WP purchased from Tani Sejati Agricultural Store (Malang, Indonesia).

### 2.2 CQD and TiO<sub>2</sub>/CQD Composite Synthesis

CQD synthesis is carried out by hydrothermal method. A total of 2 mmol of citric acid powder and 6 mmol of urea were dissolved in 25 mL of DI water. The solution is stirred using a magnetic stirrer for 10 minutes at 450 rpm, then put into an autoclave and heated for 8 hours at 160°C. The CQD solution was stored in a closed container at room temperature. TiO<sub>2</sub>/CQD composite was obtained by mixing TiO<sub>2</sub> (0.2 g), DI water (40 mL), ethanol (20 mL), and CQD (3.5 mL) using a magnetic stirrer for 5 hours at 450 rpm. Then, the solution was put into an autoclave and heated for 8 hours at 100°C. The TiO<sub>2</sub>/CQD solution was washed with aqueous and centrifuged until the precipitate was formed then heated for 3 hours at 100°C.

### 2.3 Lannate Pesticide Degradation Test 25 WP

The stock solution produced by 5 mg pesticides in 50 mL of DI water was homogenized to obtain a pesticide test solution with a 100 µg/mL concentration. It taken as much as 0.2; 0.4; 0.6; 0.8; and 1 mL, then added with DI Water until 5 mL produced a standard pesticide solution concentration of 2, 4, 6, 8, and 10 µg/mL respectively. The maximum wavenumber absorption of the samples was measured using UV-Vis spectrophotometer [19], [20]. To prepare the pesticide test solutions for degradation, a total of 10 mL pesticide stock solution was added DI water until 50 mL to produce a 10 µg/mL concentration of pesticide solution. For the TiO<sub>2</sub>/CQD blank solution preparation, 1 mg of TiO<sub>2</sub>/CQD composite was added to 10 mL of DI water and then homogenized. Take 1 mL of solution was added DI water until 5 mL, the concentration of TiO<sub>2</sub>/CQD blank solution is 10 µg/mL.

The photocatalyst activity of TiO<sub>2</sub> and TiO<sub>2</sub>/CQD composites was tested through degradation of 10 µg/mL pesticide solution under visible light (solar simulator). Catalyst material as much as 0.1 g

mixed with 50 mL of pesticide solution. The test was performed for 150 minutes to determine the degradation rate. Every 25 minutes a pesticide solution is taken. After photodegradation, the catalyst powder is separated with a discolored pesticide solution using centrifugation at 5500 rpm for 10 minutes. Degradated pesticide solutions are measured using a UV-Vis spectrometer to determine the residual concentration of pesticides. This sample can also be used on a large scale, where the amount of composite that can be used is about 0.2% in 50 mL of water.

#### 2.4 Characterization

TiO<sub>2</sub>/CQD samples were characterized using XRD to obtain crystal structure, TEM to determine sample morphology, PL to determine optical properties in the form of luminescence intensity and energy gap, BET to determine sample porosity and UV-Vis to determine optical properties and pesticide photodegradation results.

### 3. Result and Discussion

#### 3.1. TiO<sub>2</sub>/CQD Composite Structure

Figure 1 a) is an XRD TiO<sub>2</sub> pattern and TiO<sub>2</sub>/CQD composite showing a single phase with a tetragonal anatase phase crystal structure with space group I 41/AMD. Based on the image, the peak of TiO<sub>2</sub> diffraction appears at angles of  $2\theta$  25.40°, 37.8°, 48.13°, 53.98°, 55.15°, and 62.75°, confirmed by anatase TiO<sub>2</sub> crystal data from the American Mineralogist Crystal Structure Database (AMCSD) No. 0019093 with Miller index (hkl) (101), (004), (200), (105), (211) and (204), respectively. Diffraction peaks from CQD cannot be observed in TiO<sub>2</sub>/CQD composites. This is due to the low crystallinity and low CQD content in the composite so that it cannot be observed [10].

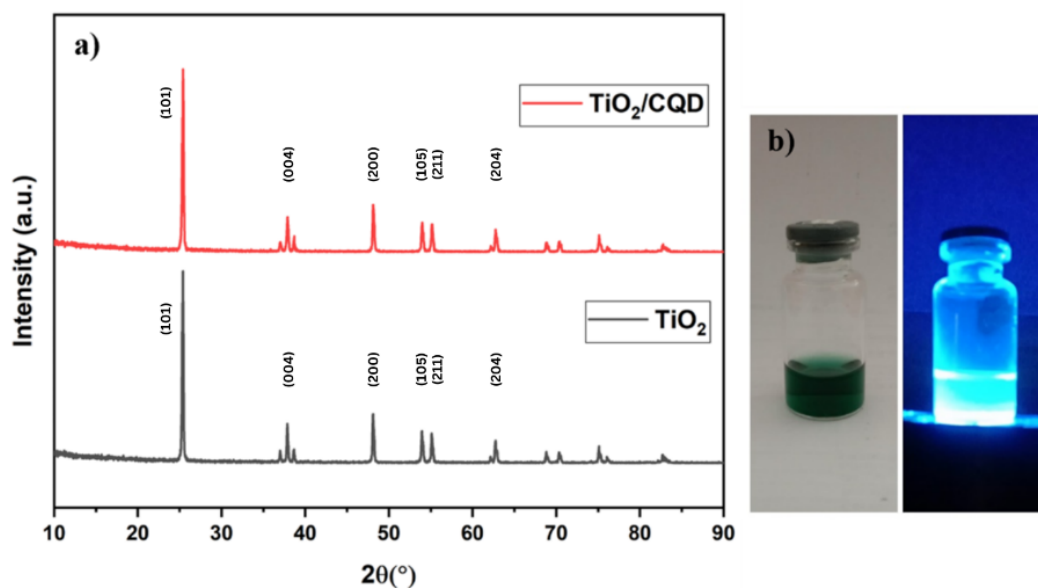


**Figure 1.** a) XRD TiO<sub>2</sub> pattern and TiO<sub>2</sub>/CQD Composite, b) CQD solution before and after UV radiation.

According to Lai, et al (2020), CQD is an amorphous phase and the diffraction peak can be observed at  $2\theta$  20–30° with the hkl (002) field [21]. However, the existence of CQD can be confirmed using TEM characterization. In addition, the TiO<sub>2</sub>/CQD did not experience a shift in diffraction peaks which showed that the addition of CQD did not influence on the purity of TiO<sub>2</sub> phase, also in accordance with previous studies [22]. These results indicate that CQD is well deposited on the TiO<sub>2</sub> surface and is not incorporated into the TiO<sub>2</sub> crystal lattice. The TiO<sub>2</sub> crystal size is 46.51 nm, after the addition of CQD the crystal size becomes smaller ~42.45 nm. Figure 1 b) represents the synthesized CQD solution. The left image is without ultraviolet (UV) irradiation, while the right image is below UV irradiation with a certain wavelength and has a luminescence indicating that CQD has successfully synthesized. Because CQD cannot be observed in the XRD diffraction pattern, TEM testing is performed to confirm the presence of CQD in TiO<sub>2</sub>/CQD composites.

#### 3.2. TiO<sub>2</sub>/CQD Composite Morphology

The morphology of the  $\text{TiO}_2/\text{CQD}$  composite is shown in Figure 2. Figure 2(a) is the morphology of the  $\text{TiO}_2/\text{CQD}$  composite with the addition of 3.5 mL of CQD. In Figure 2  $\text{TiO}_2/\text{CQD}$  composite particles have a non-uniform shape and size. The large particles are  $\text{TiO}_2$  materials, while the small particles attached to the surface of the  $\text{TiO}_2$  particles in the red circle are detected as CQD points. CQD is spherical with an average size of 5-10 nm, which is in accordance with the results of studies that have been reported [23, 24]. The image confirms the success of CQD adorning the surface of  $\text{TiO}_2$  particles. It can also be seen that there is no agglomeration in the sample. Figure 2 (b) shows the results of particle size distribution analysis using Gaussian fitting for the  $\text{TiO}_2/\text{CQD}$  composite is 114 nm. High temperature and pressure factors during the synthesis process can cause the particle size to increase by  $\sim 100$  nm. In addition, it is also influenced by the addition of CQD on  $\text{TiO}_2$  to form a composite.

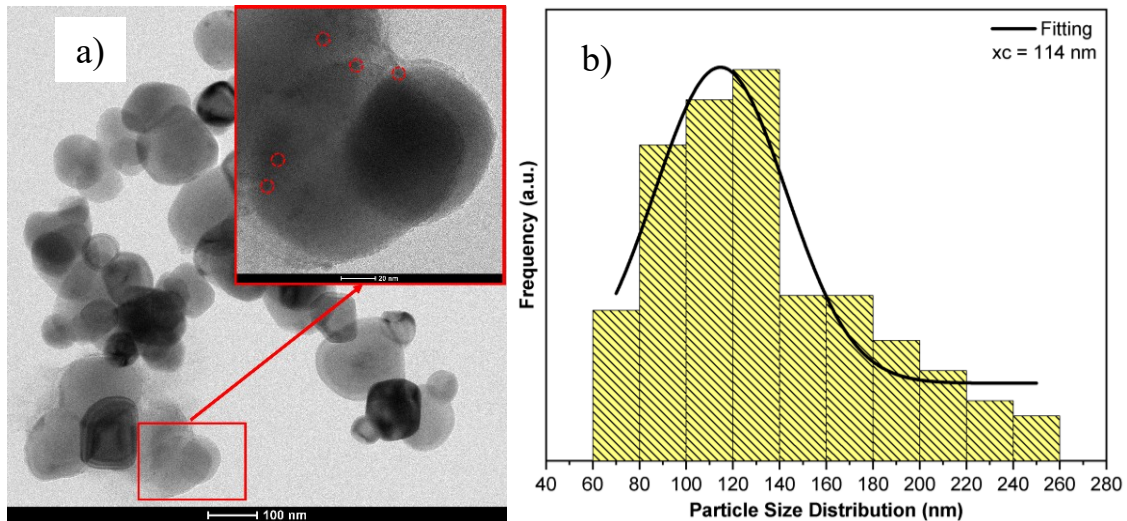


**Figure 2.** (a) TEM image of  $\text{TiO}_2/\text{CQD}$  composite (b) Particle size distribution of  $\text{TiO}_2/\text{CQD}$  composite.

### 3.3. Optical Properties of $\text{TiO}_2/\text{CQD}$ Composites

Photoluminescence (PL) characterization is carried out to determine the optical properties of the material. The PL spectra of  $\text{TiO}_2$  and the  $\text{TiO}_2/\text{CQD}$  composite were tested using an excitation wavelength of 420 nm as shown in Figure 3. The role of CQD can be known during the photocatalysis process through the PL spectra results of the  $\text{TiO}_2/\text{CQD}$  composite.

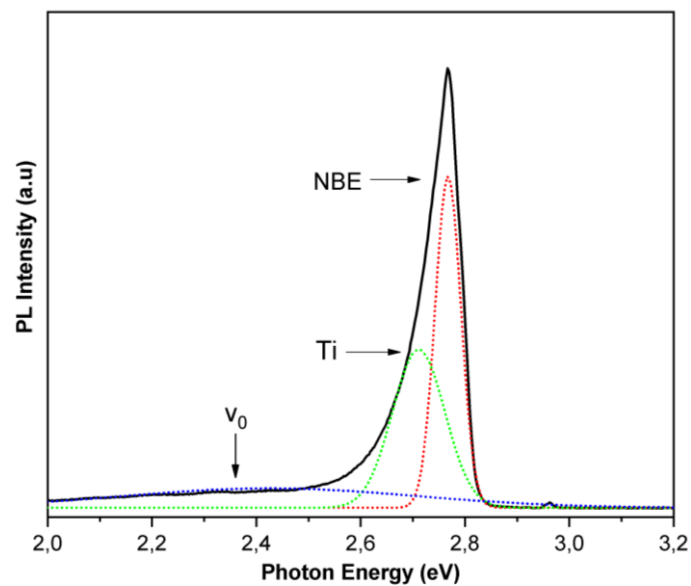


**Figure 3.**  $\text{TiO}_2/\text{CQD}$  Composite Photoluminescence Spectrum.

In Figure 3, irradiation of light with an excitation wavelength of 420 nm causes the PL  $\text{TiO}_2$  spectrum to show emission peaks at wavelengths of 450 nm (2.75 eV).  $\text{TiO}_2/\text{CQD}$  with the addition of 3.5 mL CQD has an emission peak at a wavelength of 448 nm (2.76 eV). Both  $\text{TiO}_2$  and  $\text{TiO}_2/\text{CQD}$  exhibit purple emissions, associated with band edge free actionation and shallow trap state. The three peaks in the figure showed the highest peak as Near Band Edge (NBE), the second peak as interstitial Ti ( $\text{Ti}_i$ ), and the low peak as oxygen void ( $\text{V}_0$ ). NBE emission intensity increased with the addition of CQD, while  $\text{Ti}_i$  intensity decreased. The peak of the NBE undergoes a small shift towards the wavelength of visible light, indicating a reduction in bandgap energy. Low intensity variations in the  $\text{TiO}_2/\text{CQD}$  composite show a decrease in the rate of photogeneration carrier recombination, due to increased formation of oxygen vacuums [25]. The oxygen vacuum acts as an electron trap [26], while CQD settle on the surface of  $\text{TiO}_2$  is efficient in inhibiting fot-induced electrons. CQD acts as a charge separator, increasing the electron-hole lifetime [27].  $\text{TiO}_2$  is not excited under visible light, but CQD can be excited, acting as an electron donor, while  $\text{TiO}_2$  acts as an electron acceptor [28]. NBE peaks of 2.76 eV,  $\text{Ti}_i$  of 2.70 eV, and  $\text{V}_0$  of 2.43 eV, indicating low electron-hole recombination rates, supporting photocatalytic activity.

### 3.4. Porosity of $\text{TiO}_2/\text{CQD}$ Composites

Nitrogen adsorption-desorption characterization is performed to measure the surface area and porosity of a material. The test was carried out using liquid  $\text{N}_2$  gas at a temperature of 77 °K. The method used to calculate the surface area is the Brunauer-Emmet-Teller (BET). Figure 4 is the result of  $\text{N}_2$  adsorption-desorption analysis and pore size distribution (insert) of  $\text{TiO}_2$  and  $\text{TiO}_2/\text{CQD}$  composites with the addition of 3.5 mL CQD.

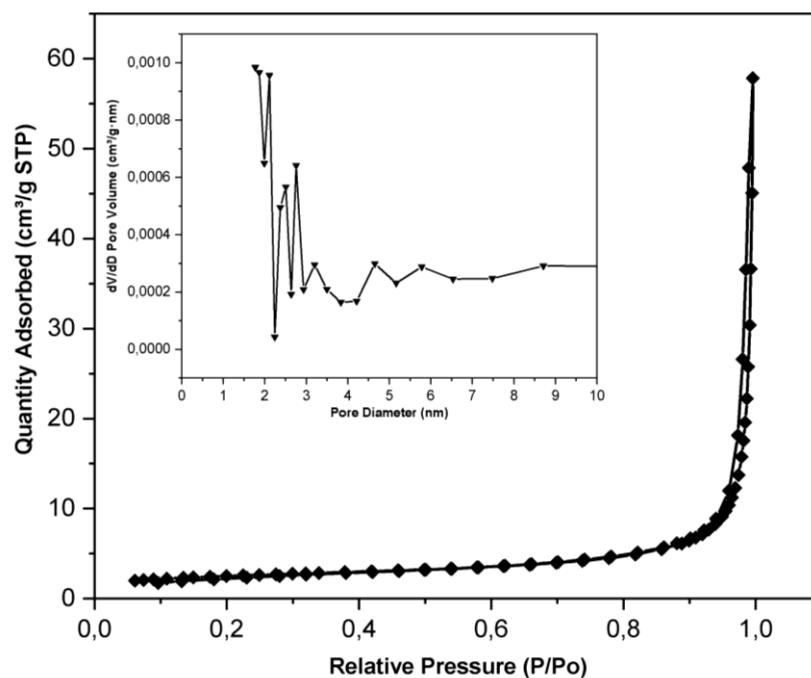


**Figure 4.** Adsorption-desorption  $\text{N}_2$  isotherms and pore size distribution curves (inserts) of the sample.

Based on the IUPAC isotherm adsorption classification, the sample showed characteristics of type IV isotherms characterized by hysteresis loops. The insert image shows an inhomogeneous pore size indicated by several peaks formed. Pore size was analyzed using the BJH method and obtained 37.4 nm. The surface area obtained is 8.6710  $\text{m}^2/\text{g}$ . In addition, a pore volume of 0.0754  $\text{cm}^3/\text{g}$  was also obtained.

### 3.5. Photocatalyst Activity of Pesticide Degradation

Standard pesticide solutions are first measured for absorbance using a UV-Vis spectrophotometer to determine the maximum wavelength. Maximum wavelength absorption measurements are carried out running from 200-700 nm wavelengths.

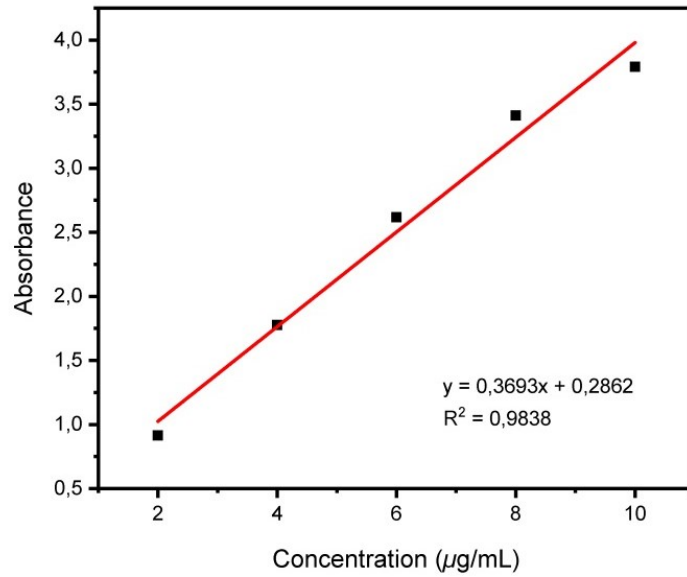


**Figure 5.** Curve of Pesticide Standard Solution

Standard pesticide solution with concentration series of 2 µg/mL, 4 µg/mL, 6 µg/mL, 8 µg/mL, and 10 µg/mL. The running results showed the optimal wavelength of the pesticide standard was at a wavelength of 235 nm. The higher the concentration used is directly proportional to the absorption value. The calibration curve of the standard solution is  $y = 0.3693x + 0.2862$ , then used to determine the % degradation value.

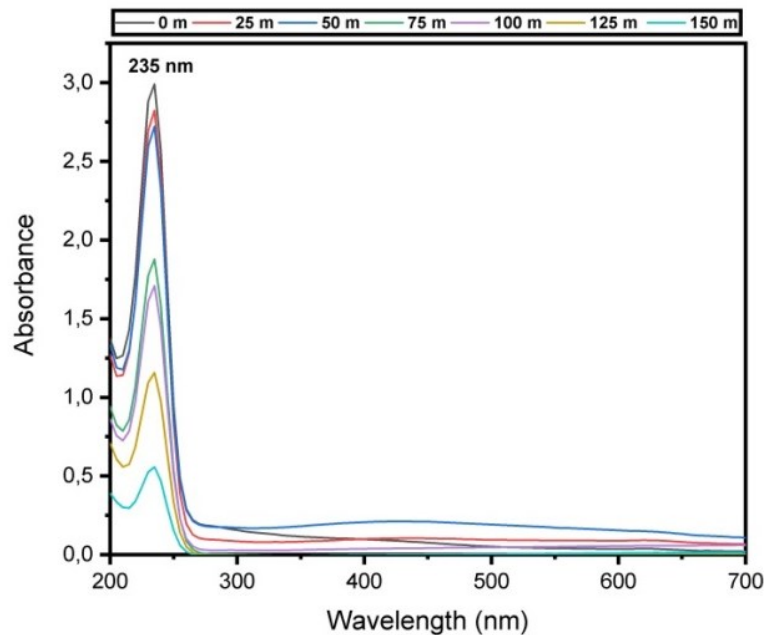


**Figure 6.** UV-Vis spectrum of pesticide degradation using TiO<sub>2</sub>/CQD composite

Figure 7a) shows the results of photocatalytic activity analysis of TiO<sub>2</sub>/CQD composites against pesticides. After 150 minutes of visible light, the pesticide was degraded by 89.9667% by TiO<sub>2</sub>/CQD. As it is known that TiO<sub>2</sub> can work effectively under UV light, which in accordance with the results of previous studies, TiO<sub>2</sub> managed to degrade MB dye up to 96% [29]. The degradation of pesticides gradually increases over time, its means that the catalytic activity of TiO<sub>2</sub>/CQD is effective using sunlight. In the early stages the adsorption process occurs rapidly because more active surface sites of the catalyst material are still empty. Over time, the active site decreases so the reaction will slow down gradually [30, 31] as shown in Figure 7. Figure 7b) is a photo of pesticide decoloration using TiO<sub>2</sub>/CQD

composites. The analysis showed that the presence of TiO<sub>2</sub>/CQD photocatalyst material succeeded in degrading pesticides under periodic visible light illumination for 150 minutes. The excellent photocatalytic activity of TiO<sub>2</sub>/CQD is associated with the interaction between CQD and TiO<sub>2</sub>. The main factors for improving photocatalytic performance are electron transfer and holes. Where CQD in TiO<sub>2</sub>/CQD composite plays a role in increasing charge transfer from photocatalyst materials to absorb the visible light optimally [22].

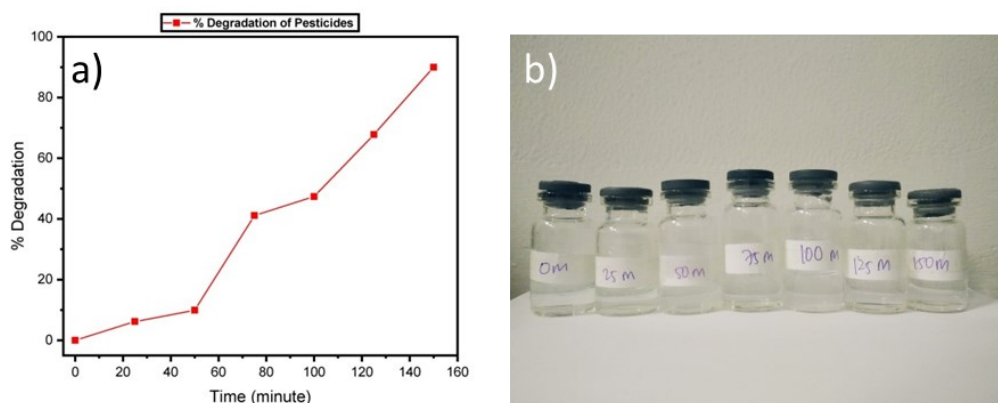


Figure 7. a) Photocatalytic activity of TiO<sub>2</sub> and TiO<sub>2</sub>/CQD composites, b) Pesticide decoloration photoage using TiO<sub>2</sub>/CQD composites

#### 4. Conclusion

The addition of CQD to the TiO<sub>2</sub>/CQD composite did not shift the XRD diffraction peak, indicating a fixed TiO<sub>2</sub> phase purity. However, the size of TiO<sub>2</sub> crystals decreases after the addition of CQD. Although there are no visible peaks of CQD in the XRD diffraction pattern, their presence is confirmed through TEM, showing good deposition with a particle size of 109-114 nm. Its optical properties were revealed through PL analysis, where the addition of CQD increased the intensity of NBE emissions, while Ti<sub>i</sub> decreased in intensity. The peak of the NBE undergoes a small shift, indicating a reduction in bandgap energy, and the intensity of V<sub>0</sub> emissions decreases, indicating an increase in the formation of oxygen vacuums. BET characterization revealed a surface area of 8.6710 m<sup>2</sup>/g, a pore diameter of 37.4 nm, and a pore volume of 0.0754 cm<sup>3</sup>/g on a TiO<sub>2</sub>/CQD composite. Porosity influences photocatalytic activity, and test results show an increase in photocatalytic activity after 150 minutes to 89.9667%. These results indicate that TiO<sub>2</sub>/CQD photocatalysts have significant potential in water treatment applications, especially in addressing pesticide contamination.

#### Acknowledgment

The authors would like to appreciate Universitas Negeri Malang which provides the facilities to conduct the research and DRTPM through the research grant scheme PTM with contract number of 20.6.84/UN32.20.1/LT/2023.

#### References

- [1] S. V. Carneiro *et al.*, "Sensing strategy based on Carbon Quantum Dots obtained from riboflavin for the identification of pesticides," *Sensors Actuators, B Chem.*, vol. 301, no. September, p. 127149, 2019, doi: 10.1016/j.snb.2019.127149.
- [2] J. G. L. Ferreira, W. H. Takarada, and E. S. Orth, "Waste-derived biocatalysts for pesticide degradation," *J. Hazard. Mater.*, vol. 427, no. September 2021, 2022, doi: 10.1016/j.jhazmat.2021.127885.
- [3] S. J. Phang and L. L. Tan, "Recent advances in carbon quantum dot (CQD)-based two dimensional materials for photocatalytic applications," *Catal. Sci. Technol.*, vol. 9, no. 21, pp. 5882–5905, 2019, doi: 10.1039/c9cy01452g.
- [4] I. Ahmad *et al.*, "ZnO and Ni-doped ZnO photocatalysts: Synthesis, characterization and improved visible light driven photocatalytic degradation of methylene blue," *Inorganica Chim. Acta*, vol. 543, no. April, p. 121167, 2022, doi: 10.1016/j.ica.2022.121167.
- [5] N. Mufti, I. K. R. Laila, Hartatiek, and A. Fuad, "The effect of TiO<sub>2</sub> thin film thickness on self-

- cleaning glass properties,” *J. Phys. Conf. Ser.*, vol. 853, no. 1, 2017, doi: 10.1088/1742-6596/853/1/012035.
- [6] M. Jeyaraj, R. Atchudan, S. Pitchaimuthu, T. N. J. I. Edison, and P. Sennu, “Photocatalytic degradation of persistent brilliant green dye in water using CeO<sub>2</sub>/ZnO nanospheres,” *Process Saf. Environ. Prot.*, vol. 156, pp. 457–464, 2021, doi: 10.1016/j.psep.2021.10.033.
- [7] Q. Guo, C. Zhou, Z. Ma, and X. Yang, “Fundamentals of TiO<sub>2</sub> Photocatalysis: Concepts, Mechanisms, and Challenges,” *Adv. Mater.*, vol. 31, no. 50, pp. 1–26, 2019, doi: 10.1002/adma.201901997.
- [8] C. Thambiliyagodage, “Activity enhanced TiO<sub>2</sub> nanomaterials for photodegradation of dyes - A review,” *Environ. Nanotechnology, Monit. Manag.*, vol. 16, no. August, p. 100592, 2021, doi: 10.1016/j.enmm.2021.100592.
- [9] S. Malmir, A. Karbalaeei, M. Pourmadadi, J. Hamedi, F. Yazdian, and M. Navaee, “Antibacterial properties of a bacterial cellulose CQD-TiO<sub>2</sub> nanocomposite,” *Carbohydr. Polym.*, vol. 234, no. July 2019, p. 115835, 2020, doi: 10.1016/j.carbpol.2020.115835.
- [10] M. S. Kumar, K. Y. Yasoda, D. Kumaresan, N. K. Kothurkar, and S. K. Batabyal, “TiO<sub>2</sub>-carbon quantum dots (CQD) nanohybrid: Enhanced photocatalytic activity,” *Mater. Res. Express*, vol. 5, no. 7, 2018, doi: 10.1088/2053-1591/aacbb9.
- [11] H. W. Chu, B. Unnikrishnan, A. Anand, Y. W. Lin, and C. C. Huang, “Carbon quantum dots for the detection of antibiotics and pesticides,” *J. Food Drug Anal.*, vol. 28, no. 4, pp. 539–557, 2020, doi: 10.38212/2224-6614.1269.
- [12] R. Behnood and G. Sodeifian, “Synthesis of N doped-CQDs/Ni doped-ZnO nanocomposites for visible light photodegradation of organic pollutants,” *J. Environ. Chem. Eng.*, vol. 8, no. 4, 2020, doi: 10.1016/j.jece.2020.103821.
- [13] H. Widiyandari *et al.*, “Nitrogen-doped carbon quantum dots supported zinc oxide (ZnO/N-CQD) nanoflower photocatalyst for methylene blue photodegradation,” *Results Eng.*, vol. 17, no. September 2022, p. 100814, 2023, doi: 10.1016/j.rineng.2022.100814.
- [14] Y. Zhou *et al.*, “Carbon Quantum Dot/TiO<sub>2</sub> Nanohybrids: Efficient Photocatalysts for Hydrogen Generation via Intimate Contact and Efficient Charge Separation,” *ACS Appl. Nano Mater.*, vol. 2, no. 2, pp. 1027–1032, 2019, doi: 10.1021/acsanm.8b02310.
- [15] X. Sun *et al.*, “Ternary TiO<sub>2</sub>/WO<sub>3</sub>/CQDs nanocomposites for enhanced photocatalytic mineralization of aqueous cephalixin: Degradation mechanism and toxicity evaluation,” *Chem. Eng. J.*, vol. 412, no. December 2020, p. 128679, 2021, doi: 10.1016/j.cej.2021.128679.
- [16] J. Korram, L. Dewangan, R. Nagwanshi, I. Karbhal, K. K. Ghosh, and M. L. Satnami, “A carbon quantum dot-gold nanoparticle system as a probe for the inhibition and reactivation of acetylcholinesterase: Detection of pesticides,” *New J. Chem.*, vol. 43, no. 18, pp. 6874–6882, 2019, doi: 10.1039/c9nj00555b.
- [17] S. Tong *et al.*, “Preparation of carbon quantum dots/TiO<sub>2</sub> composite and application for enhanced photodegradation of rhodamine B,” *Colloids Surfaces A Physicochem. Eng. Asp.*, vol. 648, no. April, p. 129342, 2022, doi: 10.1016/j.colsurfa.2022.129342.
- [18] A. Mozdbar, A. Nouralishahi, S. Fatemi, and F. S. Talatori, “The impact of Carbon Quantum Dots (CQDs) on the photocatalytic activity of TiO<sub>2</sub> under UV and visible light,” *J. Water Process Eng.*, vol. 51, no. September 2022, p. 103465, 2023, doi: 10.1016/j.jwpe.2022.103465.
- [19] A. R. Ahmad, J. Juwita, and S. A. D. Ratulangi, “Penetapan Kadar Fenolik dan Flavonoid Total Ekstrak Metanol Buah dan Daun Patikala (*Etlingera elatior* (Jack) R.M.SM),” *Pharm. Sci. Res.*, vol. 2, no. 1, pp. 1–10, 2015, doi: 10.7454/psr.v2i1.3481.
- [20] Y. Liu, S. Wei, and M. Liao, “Optimization of ultrasonic extraction of phenolic compounds from *Euryale ferox* seed shells using response surface methodology,” *Ind. Crops Prod.*, vol. 49, pp. 837–843, 2013, doi: 10.1016/j.indcrop.2013.07.023.
- [21] X. Lai *et al.*, “Hydrothermal synthesis and characterization of nitrogen-doped fluorescent carbon quantum dots from citric acid and urea,” *Ferroelectrics*, vol. 566, no. 1, pp. 116–123, 2020, doi: 10.1080/00150193.2020.1762435.
- [22] I. B. I. Williams, E. K. Fodjo, K. Amadou, T. Albert, and C. Kong, “Enhancing the photocatalytic activity of TiO<sub>2</sub> nanoparticles using green Carbon quantum dots,” *Int. J. Nano Dimens.*, vol. 13, no. 2, pp. 144–154, 2022.
- [23] F. Zheng, Z. Wang, J. Chen, and S. Li, “Synthesis of carbon quantum dot-surface modified P25

- nanocomposites for photocatalytic degradation of p-nitrophenol and acid violet 43,” *RSC Adv.*, vol. 4, no. 58, pp. 30605–30609, 2014, doi: 10.1039/c4ra02707h.
- [24] Y. Mi, N. Wang, X. Fang, J. Cao, M. Tao, and Z. Cao, “Interfacial polymerization nanofiltration membrane with visible light photocatalytic self-cleaning performance by incorporation of CQD/TiO<sub>2</sub>,” *Sep. Purif. Technol.*, vol. 277, no. July, p. 119500, 2021, doi: 10.1016/j.seppur.2021.119500.
- [25] S. Chen, Y. Xiao, Y. Wang, Z. Hu, H. Zhao, and W. Xie, “A facile approach to prepare black TiO<sub>2</sub> with oxygen vacancy for enhancing photocatalytic activity,” *Nanomaterials*, vol. 8, no. 4, pp. 1–16, 2018, doi: 10.3390/nano8040245.
- [26] B. Santara, P. K. Giri, K. Imakita, and M. Fujii, “Evidence for Ti interstitial induced extended visible absorption and near infrared photoluminescence from undoped TiO<sub>2</sub> nanoribbons: An in situ photoluminescence study,” *J. Phys. Chem. C*, vol. 117, no. 44, pp. 23402–23411, 2013, doi: 10.1021/jp408249q.
- [27] G. Rajender, J. Kumar, and P. K. Giri, “Interfacial charge transfer in oxygen deficient TiO<sub>2</sub>-graphene quantum dot hybrid and its influence on the enhanced visible light photocatalysis,” *Appl. Catal. B Environ.*, vol. 224, no. November 2017, pp. 960–972, 2018, doi: 10.1016/j.apcatb.2017.11.042.
- [28] T. H. T. Vu, T. T. Lam, D. N. Dao, D. A. Van, and T. H. Huynh, “A Composite of TiO<sub>2</sub> Quantum Dots and TiO<sub>2</sub> Nanoparticles Coated on Anti-Bumping Glass Beads (TiO<sub>2</sub>QDs-TiO<sub>2</sub>NPs/GBs), with a Very Low Content of TiO<sub>2</sub> as a High Performance Photocatalyst,” *J. Chem.*, vol. 2023, 2023, doi: 10.1155/2023/3400175.
- [29] Y. K. Abdel-Monem, “Efficient nanophotocatalyst of hydrothermally synthesized anatase TiO<sub>2</sub> nanoparticles from its analogue metal coordinated precursor,” *J. Mater. Sci. Mater. Electron.*, vol. 27, no. 6, pp. 5723–5728, 2016, doi: 10.1007/s10854-016-4484-7.
- [30] K. Firanita, S. Hidayat, F. D. Ikram, S. Bahtiar, and E. Yanuar, “Green Synthesis AgNPs Immobilized on Whatman Paper Using *Chromolaena odorata* Extract and Its Application as Photocatalyst,” *JPSE (Journal Phys. Sci. Eng.)*, vol. 7, no. 1, pp. 6–15, 2022, doi: 10.17977/um024v7i12022p006.
- [31] R. M. Kumari, N. Thapa, N. Gupta, A. Kumar, and S. Nimesh, “Antibacterial and photocatalytic degradation efficacy of silver nanoparticles biosynthesized using *Cordia dichotoma* leaf extract,” *Adv. Nat. Sci. Nanosci. Nanotechnol.*, vol. 7, no. 4, 2016, doi: 10.1088/2043-6262/7/4/045009.